

# An interferometric journey around massive stars

Anthony Meilland and Philippe Stee

Laboratoire Lagrange UMR7293 OCA - CNRS - UNS - Bd de l'Observatoire, Nice, France  
email: ame@oca.eu

**Abstract.** Since the construction in the late nineties of modern facilities such as the VLTI or CHARA, interferometry became a key technique to probe massive stars and their often-complex circumstellar environments. Over the last decade, the development of a new generation of beam combiners for these facilities enabled major breakthroughs in the understanding of the formation and evolution of massive stars. In this short review, we will present few of these advances concerning young stellar objects, binarity, mass loss, and stellar surfaces.

**Keywords.** techniques: interferometric, stars: binaries (including multiple): close, stars: circumstellar matter, stars: early-type, stars: emission-line, Be, stars: mass loss, stars: imaging

---

## 1. Introduction

Interferometry is the only observational technique allowing to spatially resolved structures smaller than the milliarcsecond, and that is not going to change soon. Actually, even the upcoming ELTs would have only one tenth of the current spatial resolution of CHARA (and one quarter of the VLTI).

Nevertheless, even if interferometry is the technique providing the highest spatial resolution, one interferometric observation only gives a very sparse knowledge of an object through the measurement of one or a few spatial frequencies of its Fourier transform. Thus, the more complex an object is, the more measurements are needed and, in that sense, interferometry is indeed a very time-consuming technique.

Another major issue with interferometric observations is the random wavefront perturbation stemming from the atmosphere. Such time-dependent perturbation makes it impossible to estimate the absolute interferometric phase. Unfortunately, this phase contains most of the information on a object as shown in Fig. 1 where either the phase or the modulus of Fourier transform is replaced by a random distribution. Despite this impossibility to directly measure the phase, partial information can be retrieve using a linear combination of the measured phases on three telescopes, called closure phase, which cancels the atmospheric contributions.

The recent increase in number of telescopes of the interferometric arrays and the improve capability of the new instruments that can simultaneously combine the light from more telescopes, with a current record of six for the MIRC instrument installed on CHARA, partly solved these issues. It allows to simultaneously measure more visibilities (up to 15) and closure phases (up to 20). With such an improvement compared to previous facilities or instruments working with two or three telescopes, better and faster sampling of the object Fourier transform can be obtained, and finally, image reconstruction techniques can be used efficiently.

In the following we will present a short review of some of the last-decade major results obtained using optical interferometry on the formation (Sect. 2), the binarity (Sect. 3), the circumstellar environment (Sect. 4), and the surface (Sect. 5) of massive stars.

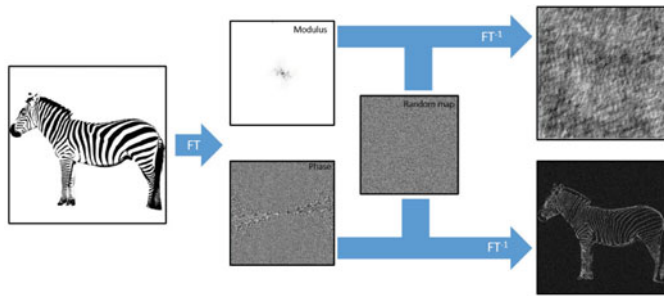


**Figure 1.** Example illustrating that most of the information on an object geometry is contained in the phase part of its Fourier transform and not in its modulus.

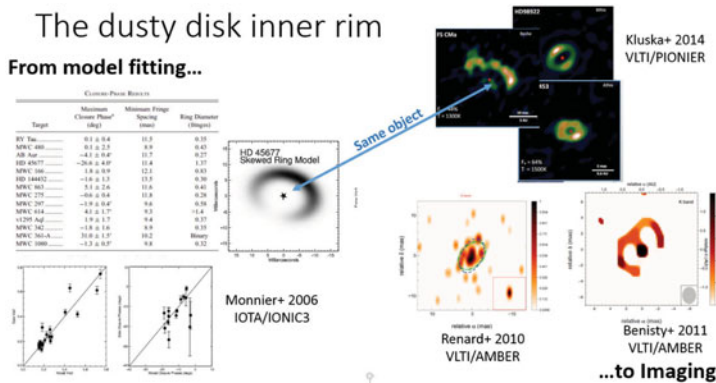


**Figure 2.** The inner rim of dusty disk around Herbig Ae/Be stars seen by optical interferometry. From Monnier *et al.* (2006), Renard *et al.* (2010), Benisty *et al.* (2011), and Kluska *et al.* (2014).

## 2. The formation of massive stars

The gain in sensibility of modern optical interferometers made it possible to observe the circumstellar environment of young stellar objects (YSO). Many studies were conducted in the near-infrared to constrain the dust sublimation radius and in the mid-infrared to probe colder material further from the central star. From PTI, IOTA, and Keck aperture masking measurements, Monnier & Millan-Gabet (2002) presented the first statistical study of the near-IR extension of YSO. This work was then completed by Keck-I measurements (Monnier *et al.* 2005) and presented in a more complete review in Dullemond & Monnier (2010). The relation they derived was compatible with simple dusty disk models with an inner rim at an expected dust sublimation temperature.

However, to discriminate between different disk models, a more detailed view of the dusty disk inner rim was needed. For instance, the measure of inner-rim skewness, that can only be done using closure phases, can help to put constraints on the inner-rim height and the disk opacity. First measurements of this skewness was done by Monnier *et al.* (2006) using IOTA. More recent facilities such as VLTI/AMBER and VLTI/PIONIER were used to obtain images of the inner-rim (Renard *et al.* 2010, Benisty *et al.* 2011, and Kluska *et al.* 2014). These results are summarized in Fig. 2.

Similar studies were conducted in the mid-infrared, mainly with the VLTI/MIDI (Leinert *et al.* 2004, Preibisch *et al.* 2006, di Folco *et al.* 2009), to probe the larger scale environment and constrain the disk density distribution, flaring, temperature law, and

chemistry thanks to MIDI high-enough spectral resolution, that allows to resolve the large PAH and silicate spectral features.

On the other hand, a higher spectral resolution was needed to resolve the hydrogen emission lines and study the geometry and kinematics of the circumstellar gas. Such studies were made possible with the VLTI/AMBER whose resolution is  $R = 1\,500$  in MR mode and  $R = 12\,000$  in HR mode. The first study was done by Malbet *et al.* (2007) on MWC 297. They showed that, for this object, the  $\text{Br}\gamma$  emission was coming from a region larger than the dusty-disk inner rim and that it was expanding, ruling out the possibility of an emission coming from an inner gaseous disk. This object was observed again by Weigelt *et al.* (2011) with a higher spectral resolution and they managed to fully model their observations with a disk-wind model. For an other object, HD 104237, Tatulli *et al.* (2007) found that the extension of the gaseous emission was of the order of the dusty disk inner rim.

The first small survey on the gaseous emission of Herbig stars was published in Kraus *et al.* (2008). They have shown that the gaseous emission can stem from various regions in the circumstellar environment. Of the five stars in their survey, two had emission originating from compact regions compatible with the inner disk. For the three others, the emission was at least as extended as the disk inner rim, favoring the hypotheses of a disk-wind or a very extended stellar wind.

Finally, the VEGA instrument, working in the visible and installed in 2008 on the CHARA array, made it possible to study the gas in the  $\text{H}\alpha$  emission line. Two objects were studied : AB Aur by Rousselet-Perraut *et al.* (2010) and HD 200775 by Benisty *et al.* (2013). They both show an extended gaseous emission compatible with a wind model, but highly flattened in the case of AB Aur.

All these previously-cited studies concern stars up to about  $10 M_{\odot}$ . The formation processes of the more massive stars are still high debated. Actually, two main scenarios are competing to explain their formation. One is a scaled-up version of Herbig stars scenario, an accretion disk phase followed by a blow-up of the remaining material by the stellar wind. The second one called “competitive accretion”, involves a high stellar density (cluster cores), which attracts and forces accretion onto the most massive stars. In this scenario all massive stars should belong to multiple systems. The first very massive young stars observed with the VLTI/AMBER (Kraus *et al.* 2010) showed no clue of binarity and a disk-like structure compatible with the first scenario (see Fig. 3). However, such result need to be confirmed on a larger sample of massive young stellar object, and the binary fraction of massive stars should also be measured.

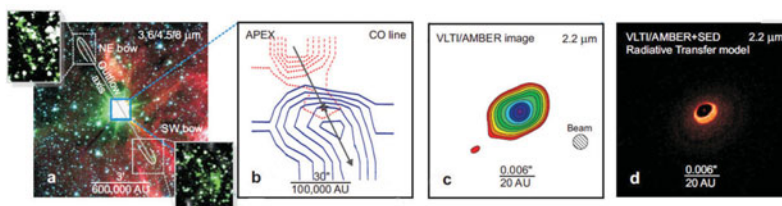


**Figure 3.** Zoom in on the massive star IRAS 13481-6124 (Kraus *et al.* 2010). From left to right: Spitzer and APEX images showing a bipolar outflow, VLTI/AMBER image and corresponding best-fit radiative model showing a disk like structure perpendicular to the outflow.

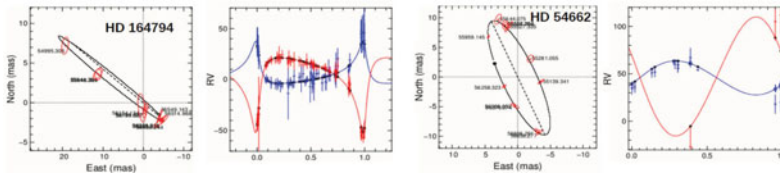


**Figure 4.** Examples of two massive stars 3D-orbit constrained using interferometric and radial velocity measurements. From yet unpublished VLTI/PIONIER data.

### 3. The multiplicity of massive stars

Optical interferometry is also a suitable technique for studying stellar multiplicity, especially when it comes to systems with separation of the order of the milliarcsecond. For instance, in an attempt to determine the binary ratio of massive stars, a joint program using the VLTI/PIONIER for small separation (1 to 45 mas) and the VLT/NACO for larger separation (30 mas to 8") was initiated. 173 southern O stars were observed during this Southern Massive stArs at High Angular Resolution (SMASH+) program. The results of this survey, published in Le Bouquin (2014), showed a very high binary fraction of the sample, 0.86, with an average number of companions of  $1.83 \pm 0.32$ . They conclude that almost all massive stars are in multiple systems.

Optical interferometry can also be used to determine the visual orbit of binary systems (i.e. projected onto the sky-plane). Combined with spectroscopic measurements of radial velocity, the full three-dimensional orbit of the system can be constrained. This allows to derive the total mass of the system and of the masses of its components with a precision down to a few percents. Many works has been done on massive binary systems, for instance: Sana *et al.* (2013) on the triple O system HD 150136 using the VLTI/PIONIER, Kraus *et al.* (2009) on the binary YSO  $\theta^1$  Ori C with the VLTI/AMBER, or Monnier *et al.* (2011) of the Wolf-Rayet binary WR104 using CHARA/CLASSIC and IOTA/IONIC3. Figure 4 presents the case of two massive stars recently observed with the VLTI/PIONIER.

During their evolution, stars in binary systems can interact with each other through their circumstellar or circumbinary environment. Such interactions, that can be once again well constrained using optical interferometry, are mainly due to gravitational effects or particle collisions (mainly in stellar winds).

The Be-binary system  $\beta$  Lyr is a good example of what can be done on interacting systems using interferometry . This semidetached binary is composed of two B-type stars, a primary supergiant filling its Roche lobe, and a secondary surrounded by an accretion disk fed by the primary material leaking in through the system's first Lagrangian point. Near-infrared reconstructed-images during a complete orbital period were obtained by Zhao *et al.* (2008) using the CHARA/MIRC combiner (see Fig. 5). On these images two components are seen, one unresolved, the primary, and one elongated, the secondary surrounded by the accretion disk. To go further in this study, and disentangle the stellar and circumstellar emission, the system was also observed in  $H\alpha$  with the CHARA/VEGA instrument (Bonneau *et al.* 2011). The authors found that the emission was coming from a structure larger than the binary separation, most probably a circumbinary disk with possible contributions from polar jets.

Another interacting binary system discovered and studied using interferometry is the yellow hypergiant HR 5171A. Chesneau *et al.* (2014) showed that this star, one of the largest known star, i.e.  $R \sim 1300 R_{\odot}$ , is in contact with a previously unknown companion, and that the system is probably in a common envelope phase.

Due to a lack of sensibility, only a few studies of wind collisions were conducted using interferometry. The main results were obtained with the Keck aperture masking

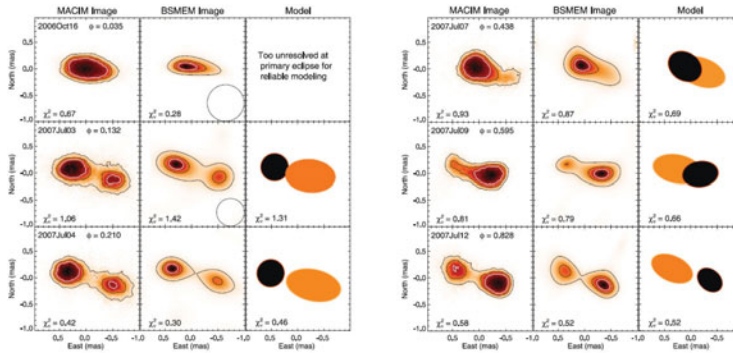


**Figure 5.** The Be-binary system  $\beta$  Lyr as seen by CHARA/MIRC during one full orbital period. From Zhao *et al.* (2008).

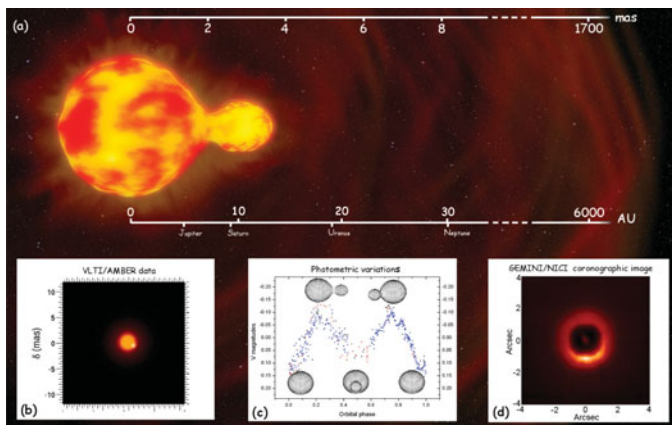


**Figure 6.** VLT/AMBER observations and long term photometry revealed the binary nature and common envelope phase of the yellow hypergiant HR 5171A. From Chesneau *et al.* (2014).

experiment (Tuthill *et al.* 1999, Harries *et al.* 2004 and Monnier *et al.* 2007a) on imaging of dust around Wolf-Rayet stars. They found out that the dust was located in a pinwheel nebulae, i.e. a spiral-like pattern tracing the orbital motion of the wind-collision layer. The first Wolf-Rayet stars observed with long-baseline optical interferometry were  $\gamma^2$  Vel (Millour *et al.* 2007) and WR 118 (Millour *et al.* 2009b). In both papers, the authors manage to resolve the system, and in that second one, they found closure phase signal compatible with a pinwheel model.

#### 4. Mass loss and circumstellar environments

As a natural tracer of mass loss, the study of massive stars circumstellar environment is crucial to improve their evolution models. To characterize not only the total mass loss but its possible anisotropy, one has to put some constraints on the geometry and kinematics of the close surrounding of these massive stars. Interferometry and in particular spectro-interferometry are indeed powerful techniques to probe these environments whose extensions are usually of the order of few milliarcseconds in the visible and near-IR and tens of milliarcseconds in the mid-IR.

Chesneau *et al.* (2010) used the CHARA/VEGA instrument to study the wind of two blue supergiants: Deneb and Rigel. He managed to model these high-spectral resolution

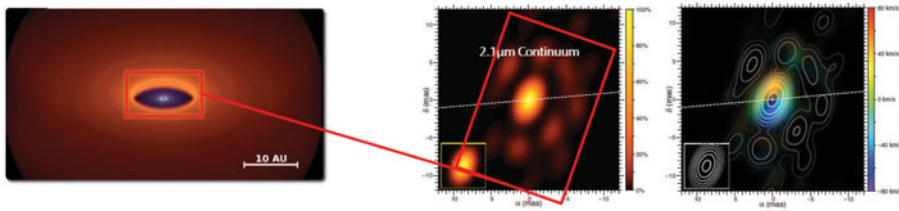


**Figure 7.** The A[e] supergiant seen by the VLTI instruments MIDI (left) and AMBER, in the  $2.1\ \mu\text{m}$  continuum (center) and the  $\text{Br}\gamma$  line (right). From Meilland *et al.* (2010) and Millour *et al.* (2011).

( $R=30000$ ) observations centered on  $\text{H}\alpha$  using the CMFGEN radiative transfer code. The authors also found a strong asymmetry in Deneb wind.

Using VLTI/AMBER and VLTI/VINCI measurements Groh *et al.* (2010) probed the heart of  $\eta$  Car circumstellar environment. They studied possible effects from fast-rotation of the primary and wind collision to explain the break of symmetry of the mass loss and the formation of the Homonculus nebula around these very massive objects. The interferometric study of  $\eta$  Car is still going on and new results are presented further in this book.

Actually, the mass-loss break of symmetry, its origin and its consequences are major issues in the understanding of stellar evolution. Binarity and rotation are the most common physical phenomena that can cause departure from a spherically symmetric mass loss, affecting the loss of angular momentum of the star itself.

Among the objects concerned by this break of symmetry are the stars showing the B[e] phenomenon, i.e. presence of forbidden lines produced in a diluted and highly illuminated medium and of strong IR-excess due to the presence of dust produced in a dense and cool medium. Both rotation through the bi-stable model and binarity were proposed to explain the formation of an equatorial structure dense enough to allow dust formation in their circumstellar environment.

These B[e] stars were perfect targets for the VLTI instruments MIDI and AMBER and the brightest of them were studied in the last decade : CPD -57°2874 (Domiciano de Souza *et al.* 2007), Hen 3-1191 (Lachaume *et al.* 2007), HD 87643 (Millour *et al.* 2009a), HD 62623 (Meilland *et al.* 2010, Millour *et al.* 2011), HD 50138 (Borges Fernandes *et al.* 2011), MWC 300 (Wang *et al.* 2012), HD 327083 (Wheelwright *et al.* 2012), V921 Sco (Kreplin *et al.* 2012), and HD 85567 (Wheelwright *et al.* 2013). Most of these study modeled either with simple geometric model or radiative transfer code such as MC3D, conclude that the dust was located in a circumstellar disk and that the gaseous emission was coming from structures smaller than the dusty-disk inner rim.

In Fig. 7 we present the results obtained on the most extensively studied object with both MIDI and AMBER : the A[e] supergiant HD 62623. For this object, the authors found that both the gas and dust formed a stratified disk in Keplerian rotation, and that the stellar velocity was too small for the rotation to explain the break of symmetry of the environment but too high for a supergiant. They concluded that this star has probably gone through a spin-up phase due to interaction with a spectroscopically detected companion. However, the detailed mechanisms for the disk formation remain unknown.

Classical Be stars were already favored targets for interferometers in the nineties. However, these studies were quite limited by the data lack of accuracy and the small number of telescopes of the interferometric arrays. In the last decade, many objects were observed with modern facilities, and data were analyzed using either simple geometric or kinematic models (Tycner *et al.* 2004, Tycner *et al.* 2006, Meilland *et al.* 2008, Delaa *et al.* 2011,

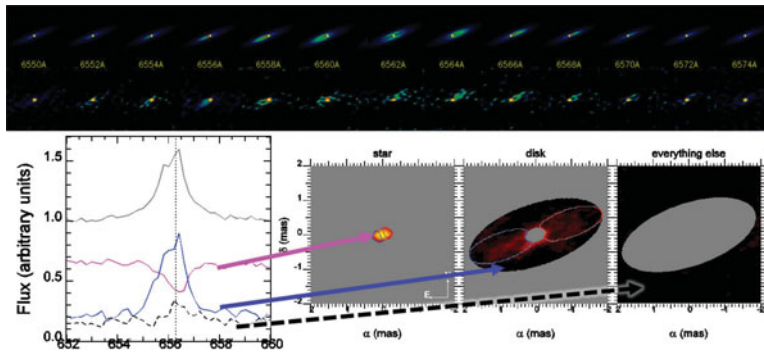


**Figure 8.** Narrow-spectral band images in the  $H\alpha$  line (top) and extracted spectrum for the star and disk (bottom) for the Be-shell star  $\phi$  Per. From CHARA/VEGA measurement to be published in Mourard *et al.* (2014).

Stee *et al.* 2012, Kraus *et al.* 2012) or radiative transfer codes such as SIMECA (Meilland *et al.* 2007a, Meilland *et al.* 2007b), BEDSIK (Tycner *et al.* 2011), or HDUST (Štefl *et al.* 2009, Carciofi *et al.* 2009). In all cases the authors found that the circumstellar emission stems from a thin equatorial disk. The more detailed studies, using spectral resolution allowed to probe the kinematics and show that disks were dominated by rotation, probably close to the Keplerian one. The disk density law was also constrained, showing that the observations were compatible with the viscous excretion disk model.

Two Be binary stars were extensively studied to understand the effect of binarity on the Be phenomenon :  $\delta$  Sco (Tycner *et al.* 2011, Meilland *et al.* 2011, Meilland *et al.* 2013) and Achernar (Kervella & Domiciano de Souza 2006, Kanaan *et al.* 2008, Kervella *et al.* 2009). Finally, some statistical studies of Be stars environments were conducted to constrain the general properties of their disks (Gies *et al.* 2007, Meilland *et al.* 2009, Touhami *et al.* 2013) and also to derive a mean rotational rate of Be stars showing that they were very close to their critical rotation (Meilland *et al.* 2012).

Fig. 8 shows an example of the possibility of Be stars observations with modern spectro-interferometric instruments. In this forthcoming paper, Mourard *et al.* (2014) manage to reconstruct narrow-spectral band images in the  $H\alpha$  line probing the disk geometry and kinematics of this Be-shell star. As shown in the figure, the technique is similar to integral-field spectroscopy but with a forty-times higher spatial resolution.

## 5. From diameters measurements to stellar imaging

Stellar radius is one of the main input parameters of stellar interior models. It is often used to derive the star mass, age and other physical parameters. With no direct angular measurements, the radius is generally inferred from photometry but with some important biases and poor accuracy. Modern interferometers allow to obtain accurate angular diameters, and using Hipparcos parallaxes, to derive more accurate linear radii.

Accurate angular diameters are also needed to calibrate the surface-brightness relation for some distance estimators such Cepheids and eclipsing binaries. Up to recently, such relation was poorly constrained for early type stars. Recently, significant improvements (see Fig. 9) were obtained using the two CHARA visible beam-combiners, PAVO (Maestro *et al.* 2013) and VEGA (Challouf *et al.* 2014).

Actually, the first star measured with interferometry almost a hundred years ago, the red supergiant Betelgeuse, is still being observed with modern facilities. Haubois *et al.* (2009) obtained the first reconstructed image of its stellar surface. He managed

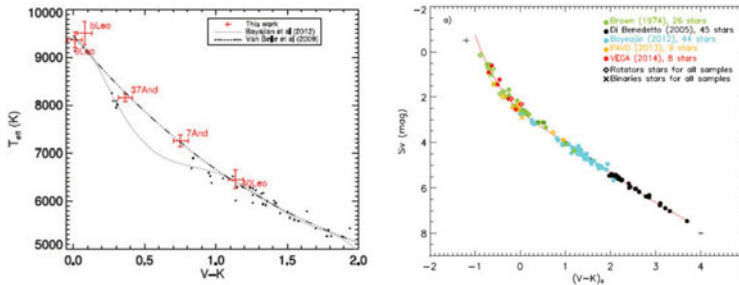


**Figure 9.** Surface brightness relation for early type stars determined with CHARA/PAVO (Maestro *et al.* 2013, left) and CHARA/VEGA (Challouf *et al.* 2014, right).

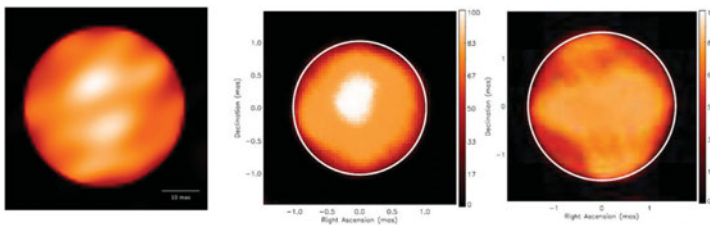


**Figure 10.** Reconstructed images of red supergiants: Betelgeuse (left), RS Per (center) and T Per (right). From Haubois *et al.* (2009) and Baron *et al.* (2014).

to detect giant “spots” on the surface that are compatible with convection cells (see Fig. 10). Two other red supergiants were imaged by (Baron *et al.* 2014) in the K-band continuum with CHARA/MIRC whereas the yellow supergiant Canopus was resolved by the VLTI/AMBER (Domiciano de Souza *et al.* 2012).

On the other hand, using the VLTI/AMBER spectro-interferometric capability, Ohnaka *et al.* (2009) resolved the  $2.3 \mu\text{m}$  CO bands of Betelgeuse. These observations allowed to study the geometry and kinematics, showing evidence of asymmetry and convection in a  $1.3 R_*$  extended atmosphere. New observations published in Ohnaka *et al.* (2011) showed significant changes in the kinematics and geometry. Similar results were found for another red supergiant, i.e. Antares (Ohnaka *et al.* 2013).

Stellar surfaces of five intermediate-mass fast-rotators were imaged in the K band using the CHARA/MIRC instrument (Monnier *et al.* 2007b, Zhao *et al.* 2009, Che *et al.* 2011). The reconstructed images, presented in Fig. 11, allowed to constrain the photosphere flattening and gravity darkening induced by the Von Zeipel effect. Actually, the authors found that their observations are better fitted by a  $\beta$  exponent of 0.22, i.e. slightly different from the 0.25 value derived in Von Zeipel work for radiative stars. Finally, using the ESTER model for interior of fast rotating stars, Espinosa Lara & Rieutord (2011) found values compatible to the one measured by MIRC.

However, Delaa *et al.* (2013) showed that the measured value of the  $\beta$  parameter can be biased in case of a latitudinal differential rotation. Such degeneracy on the gravity darkening measurement could be removed using spectro-interferometry in photospheric lines as show in Fig. 12.

Finally, the differential phase measurements can also be used to measure the stellar diameters of unresolved fast-rotators as shown by Domiciano de Souza *et al.* (2012) using VLTI/AMBER high-resolution measurements of the close-to-critical rotator Achernar. Using the same technique Hadjara *et al.* (2014) even managed to derive the radius for slower rotators.

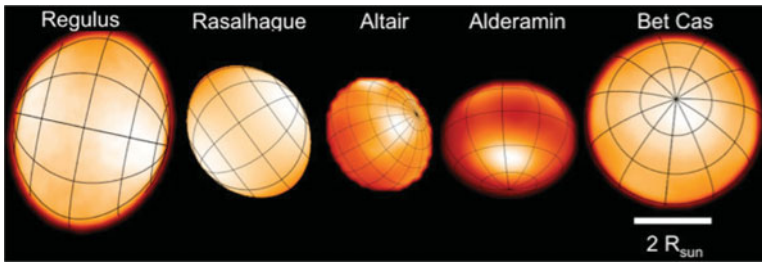


**Figure 11.** Fast rotators as seen by CHARA/MIRC. From Monnier *et al.* (2007b), Zhao *et al.* (2009), and Che *et al.* (2011).

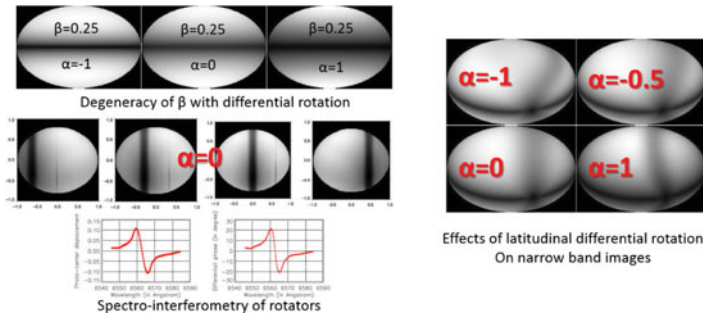


**Figure 12.** Stellar rotation probed by spectro-interferometry. Top left: Intensity map in the continuum showing the degeneracy of the  $\beta$  parameters for different values of the latitudinal-differential rotation parameter  $\alpha$ . Bottom left: Narrow band images at different wavelengths through a photopheric line for  $\alpha = 0$  and corresponding differential phase signal. Narrow band images at one wavelength for different values of the  $\alpha$  parameter. From Delaa *et al.* (2013).

## References

- Baron, F., Monnier, J. D., Kiss, L. L., *et al.* 2014, *ApJ* 785, 46  
 Benisty, M., Perraut, K., Mourard, D., *et al.* 2013, *A&A* 555, A113  
 Benisty, M., Renard, S., Natta, A., *et al.* 2011, *A&A* 531, A84  
 Bonneau, D., Chesneau, O., Mourard, D., *et al.* 2011, *A&A* 532, A148  
 Borges Fernandes, M., Meilland, A., Bendjoya, P., *et al.* 2011, *A&A* 528, A20  
 Carciofi, A. C., Okazaki, A. T., Le Bouquin, J.-B., *et al.* 2009, *A&A* 504, 915  
 Challouf, M., Nardetto, N., Mourard, D., *et al.* 2014, *Submitted to A&A*  
 Che, X., Monnier, J. D., Zhao, M., *et al.* 2011, *ApJ* 732, 68  
 Chesneau, O., Dessart, L., Mourard, D., *et al.* 2010, *A&A* 521, A5  
 Chesneau, O., Meilland, A., Chapellier, E., *et al.* 2014, *A&A* 563, A71  
 Delaa, O., Stee, P., Meilland, A., *et al.* 2011, *A&A* 529, A87  
 Delaa, O., Zorec, J., Domiciano de Souza, A., *et al.* 2013, *A&A* 555, A100  
 di Folco, E., Dutrey, A., Chesneau, O., *et al.* 2009, *A&A* 500, 1065  
 Domiciano de Souza, A., Driebe, T., Chesneau, O., *et al.* 2007, *A&A* 464, 81  
 Domiciano de Souza, A., Hadjara, M., Vakili, F., *et al.* 2012, *A&A* 545, A130  
 Dullemond, C. P. & Monnier, J. D. 2010, *ARA&A* 48, 205  
 Espinosa Lara, F. & Rieutord, M. 2011, *A&A* 533, A43  
 Gies, D. R., Bagnuolo, Jr., W. G., Baines, E. K., *et al.* 2007, *ApJ* 654, 527  
 Groh, J. H., Madura, T. I., Owocki, S. P., Hillier, D. J., & Weigelt, G. 2010, *ApJ (Letters)* 716, L223  
 Hadjara, M., Domiciano de Souza, A., Vakili, F., *et al.* 2014, *Submitted to A&A*  
 Harries, T. J., Monnier, J. D., Symington, N. H., & Kurosawa, R. 2004, *MNRAS* 350, 565  
 Haubois, X., Perrin, G., Lacour, S., *et al.* 2009, *A&A* 508, 923  
 Kanaan, S., Meilland, A., Stee, P., *et al.* 2008, *A&A* 486, 785

- Kervella, P. & Domiciano de Souza, A. 2006, *A&A* 453, 1059
- Kervella, P., Domiciano de Souza, A., Kanaan, S., *et al.* 2009, *A&A* 493, L53
- Kluska, J., Malbet, F., Berger, J.-P., *et al.* 2014, in M. Booth, B. C. Matthews, & J. R. Graham (eds.), *IAU Symposium*, Vol. 299 of *IAU Symposium*, pp 117–118
- Kraus, S., Hofmann, K.-H., Benisty, M., *et al.* 2008, *A&A* 489, 1157
- Kraus, S., Hofmann, K.-H., Menten, K. M., *et al.* 2010, *Nature* 466, 339
- Kraus, S., Monnier, J. D., Che, X., *et al.* 2012, *ApJ* 744, 19
- Kraus, S., Weigelt, G., Balega, Y. Y., *et al.* 2009, *A&A* 497, 195
- Kreplin, A., Kraus, S., Hofmann, K.-H., *et al.* 2012, *A&A* 537, A103
- Lachaume, R., Preibisch, T., Driebe, T., & Weigelt, G. 2007, *A&A* 469, 587
- Le Bouquin, J.-B. 2014, *Submitted to A&A*
- Leinert, C., van Boekel, R., Waters, L. B. F. M., *et al.* 2004, *A&A* 423, 537
- Maestro, V., Che, X., Huber, D., *et al.* 2013, *MNRAS* 434, 1321
- Malbet, F., Benisty, M., de Wit, W.-J., *et al.* 2007, *A&A* 464, 43
- Meilland, A., Delaa, O., Stee, P., *et al.* 2011, *A&A* 532, A80
- Meilland, A., Kanaan, S., Borges Fernandes, M., *et al.* 2010, *A&A* 512, A73
- Meilland, A., Millour, F., Kanaan, S., *et al.* 2012, *A&A* 538, A110
- Meilland, A., Millour, F., Stee, P., *et al.* 2007a, *A&A* 464, 73
- Meilland, A., Millour, F., Stee, P., *et al.* 2008, *A&A* 488, L67
- Meilland, A., Stee, P., Chesneau, O., & Jones, C. 2009, *A&A* 505, 687
- Meilland, A., Stee, P., Spang, A., *et al.* 2013, *A&A* 550, L5
- Meilland, A., Stee, P., Vannier, M., *et al.* 2007b, *A&A* 464, 59
- Millour, F., Chesneau, O., Borges Fernandes, M., *et al.* 2009a, *A&A* 507, 317
- Millour, F., Driebe, T., Chesneau, O., *et al.* 2009b, *A&A* 506, L49
- Millour, F., Meilland, A., Chesneau, O., *et al.* 2011, *A&A* 526, A107
- Millour, F., Petrov, R. G., Chesneau, O., *et al.* 2007, *A&A* 464, 107
- Monnier, J., Millan-Gabet, R., & Billmeier, R. 2005, *ApJ* 624, 832
- Monnier, J. D., Berger, J.-P., Millan-Gabet, R., *et al.* 2006, *ApJ* 647, 444
- Monnier, J. D. & Millan-Gabet, R. 2002, *ApJ* 579, 694
- Monnier, J. D., Tuthill, P. G., Danchi, W. C., Murphy, N., & Harries, T. J. 2007a, *ApJ* 655, 1033
- Monnier, J. D., Zhao, M., Pedretti, E., *et al.* 2011, *ApJ (Letters)* 742, L1
- Monnier, J. D., Zhao, M., Pedretti, E., *et al.* 2007b, *Science* 317, 342
- Mourard, D., Monnier, J., Che, X., Meilland, A., & Millour, F. 2014, *Submitted to A&A*
- Ohnaka, K., Hofmann, K.-H., Benisty, M., *et al.* 2009, *A&A* 503, 183
- Ohnaka, K., Hofmann, K.-H., Schertl, D., *et al.* 2013, *A&A* 555, A24
- Ohnaka, K., Weigelt, G., Millour, F., *et al.* 2011, *A&A* 529, A163
- Preibisch, T., Kraus, S., Driebe, T., van Boekel, R., & Weigelt, G. 2006, *A&A* 458, 235
- Renard, S., Malbet, F., Benisty, M., Thiébaud, E., & Berger, J.-P. 2010, *A&A* 519, A26
- Rousselet-Perraut, K., Benisty, M., Mourard, D., *et al.* 2010, *A&A* 516, L1
- Sana, H., Le Bouquin, J.-B., Mahy, L., *et al.* 2013, *A&A* 553, A131
- Stee, P., Delaa, O., Monnier, J. D., *et al.* 2012, *A&A* 545, A59
- Tatulli, E., Isella, A., Natta, A., *et al.* 2007, *A&A* 464, 55
- Touhami, Y., Gies, D. R., Schaefer, G. H., *et al.* 2013, *ApJ* 768, 128
- Tuthill, P. G., Monnier, J. D., & Danchi, W. C. 1999, *Nature* 398, 487
- Tycner, C., Ames, A., Zavala, R. T., *et al.* 2011, *ApJ (Letters)* 729, L5
- Tycner, C., Gilbreath, G. C., Zavala, R. T., *et al.* 2006, *AJ* 131, 2710
- Tycner, C., Hajian, A. R., Armstrong, J. T., *et al.* 2004, *AJ* 127, 1194
- Šteff, S., Rivinius, T., Carciofi, A. C., *et al.* 2009, *A&A* 504, 929
- Wang, Y., Weigelt, G., Kreplin, A., *et al.* 2012, *A&A* 545, L10
- Weigelt, G., Grinin, V. P., Groh, J. H., *et al.* 2011, *A&A* 527, A103
- Wheelwright, H. E., de Wit, W. J., Oudmaijer, R. D., & Vink, J. S. 2012, *A&A* 538, A6
- Wheelwright, H. E., Weigelt, G., Caratti o Garatti, A., & Garcia Lopez, R. 2013, *A&A* 558, A116

Zhao, M., Gies, D., Monnier, J. D., *et al.* 2008, *ApJ (Letters)* 684, L95

Zhao, M., Monnier, J. D., Pedretti, E., *et al.* 2009, *ApJ* 701, 209



Anthony Meilland